Research Paper

Removal of 1-Naphthol From Water via Photocatalytic Degradation Over N,S-TiO_2/Silica Sulfuric Acid Under Visible Light

Farhad Mahmoodi[1], Reza Jalilzadeh Yengejeh[1], Farhang Tirgir[2*], Mehraban Sadeghi[1,3]

1. Department of Environmental Engineering, Ahvaz Branch, Islamic Azad University, Ahvaz, Iran.
2. Department of Chemistry, Faculty of Science, Shahrekord Branch, Islamic Azad University, Shahrekord, Iran.
3. Department of Environmental Health Engineering, School of Health, Shahrekord University of Medical Sciences, Rahmatieh Shahrekord, Iran.

Use your device to scan and read the article online

Citation Mahmoodi F, Jalilzadeh Yengejeh R, Tirgir F, Sadeghi M. Removal of 1-Naphthol From Water via Photocatalytic Degradation Over N,S-TiO_2/Silica Sulfuric Acid Under Visible Light. Journal of Advances in Environmental Health Research. 2022; 10(1):59-72. http://dx.doi.org/10.32598/JAEHR.10.1.1242

http://dx.doi.org/10.32598/JAEHR.10.1.1242

Article info:
Received: 05 May 2021
Accepted: 22 Aug 2021
Publish: 01 Jan 2022

Keywords:
Water pollution, TiO_2, Photocatalytic, Degradation, 1-Naphthol

ABSTRACT

Background: Naphthol, one of the naphthalene derivatives, is the most significant industrial chemical. It is widely used in the biochemical processes, production of dyes, and pharmaceutical industries.

Methods: In the present study, N, S-doped TiO_2 thin film immobilized on Silica Sulfuric Acid (SSA) glass Microspheres (MS) was investigated as a novel high efficient photocatalyst. We fabricated N, S-doped TiO_2 immobilized on SSA using a simple modified sol-gel process. Its photocatalytic activities were then assessed by 1-naphthol solution in the presence of visible light. The physicochemical properties of photocatalyst were characterized using Energy-Dispersive X-ray (EDX), Scanning Electron Microscope (SEM) images, and X-Ray Diffraction (XRD) pattern.

Results: According to the obtained results, the optimal pH, time, concentration, and removal efficiency of 1-naphthol for N, S-doped TiO_2 /SSA were 5, 50 min, 25 mg/L, and 92.12%.

Conclusion: The present study confirms the usability of the immobilized N, S-doped TiO_2 on SSA glass MS as a novel, effective, and efficient technique for treating wastewater containing 1-naphthol under visible light.

*** Corresponding Author:**
Farhang Tirgir, PhD.
Address: Department of Chemistry, Faculty of Science, Shahrekord Branch, Islamic Azad University, Shahrekord, Iran.
Phone:+98(913)2076307
E-mail: tirgir588@gmail.com ; tirgir588@gmail.com

1. Introduction

Phenols are among the important pollutants listed by the US Environmental Protection Agency and the European Union [1]. 1-Naphthol, one of the derivatives of naphthalene, is the most significant industrial chemical that is widely used in the production of dyes, pharmaceuticals, and biochemical processes [2]. Because of its oxidation through chemical and biological processes, naphthalene (the main coal tar constituent) enters the environment [3]. The presence of hydroxyl group in the backbone of 1-naphthalene increases its solubility and mobility in natural aquifers. 1-Naphthalene toxicity is higher than naphthalene and derived aromatic hydrocarbons [4]. Various treatment methods for wastewater containing phenolic compounds have been investigated using chemical and biological methods [5, 6].

Nevertheless, the aforementioned methods have their limitations and disadvantages [7]. Recently, new advanced oxidation processes have been considered [8-12]. Titanium dioxide (TiO_2) as a semiconductor is a highly effective and reflective catalyst compared to other semiconductors. TiO_2 is non-toxic, photo corrosion-resistant, cheap, and suitable for working with sunlight. Pure TiO_2 is a weak photon absorber within the visible part of the solar spectrum because of its large distance of the energy bond (Anatase; 3.2 eV, Rutile; 3.05 eV) [13-16]. This property has led to the development of TiO_2 nanoparticles with several novel strategies to alter their ultraviolet and optical response to the visible spectral range so that visible light can be efficiently used in the solar spectrum main part [17]. Therefore, some methods like noble metals and anions (S, F, N, C)-doping are being used to convert this inherent property of TiO_2 and produce a new photocatalyst capable of maintaining its photocatalytic activity under sunlight [18-20]. Sulfur anions-nitrogen doped with TiO_2 creates a gap between the two capacitance bands and a narrower conductivity, leading to adsorption in the visible region [21].

Recently, TiO_2 powder nanoparticles have been extensively used. Many studies report that the TiO_2 photocatalysts are immobilized on surfaces such as glass Microspheres (MS) [22, 23], silica [24], zeolites, and nanotubes because of problems such as repetitive mixing throughout work, the expensive filtration and centrifugation of solutions for catalyst recovery, nanoparticles dispersion in solution and blockage of light, and the like. In the literature, the use of glass beads for catalyst deposition has been of considerable interest [25, 26]. In this study, the new catalyst N, S-TiO_2 coated on Silica Sulfuric Acid (SSA) was prepared. The SSA was synthesized according to previous studies and should be prepared by reaction of silica glass beads with chlorosulfonic acid [27]. The immobilized N,S-TiO_2 nanoparticles on SSA were evaluated using Energy-Dispersive X-ray (EDX), Scanning Electron Microscope (SEM), and X-Ray Diffraction (XRD). In addition, the optimal removal conditions of 1-naphthol are investigated using pH, irradiation time, and 1-naphthol concentration under visible light. Then, 1-naphthol removal reaction kinetics is measured.

2. Materials and Methods

Synthesis of photocatalyst

The chemicals used in the experiments were obtained without further purification. 1-Naphthol was obtained from Merck Co. in Germany. The water employed in all studies was double distilled. Because of the immobilization of the prepared sol of tetrabutyl orthotitanate on a substrate, the glass MS with 500 µ in diameter made of glass beads was used. SSA was prepared according to previous studies [27] through silica glass beads reaction with chlorosulfonic acid (Figure 1). N,S-TiO_2 thin film coated on SSA was prepared via tetrabutyl orthotitanate hydrolysis in the presence of SSA instead of glass beads using the sol-gel method following previous work.

Study of photocatalyst properties

The crystallinity and particle size of the prepared N,S-TiO_2 thin film on SSA and pure SSA (as compared) were studied using XRD patterns gathered within the range of 20-80 (2θ) with a Philips X (X-Ray Tube Anode: Cu Wavelength: 1.540598 °A [Cu Kα] Filter: Ni). Using the Scherrer equation, the mean size of crystalline particles of the anatase phase was calculated. The bandgap of N,S-TiO_2/SSA was calculated by UV-Vis with Shimadzu UV-1800 spectrophotometer and compared with a band gap of N,S-TiO_2 coated on glass beads. The surface morphology of N,S-TiO_2 thin film on SSA was investigated using Zeiss EVO 15 SEM equipped with an XRD spectrometer to analyze its elements.

Optical activity of photocatalyst investigation

In the experiments, 1 g of 1-naphthol was dissolved in 500 mL of naturally distilled water (pH 7) and diluted to 1000 mL to prepare different solution concentrations. The solution was spun using a peristaltic pump within a reactor with a flow rate of 20 mL/min. The primary concentrations of 1-naphthol solution were as follows:

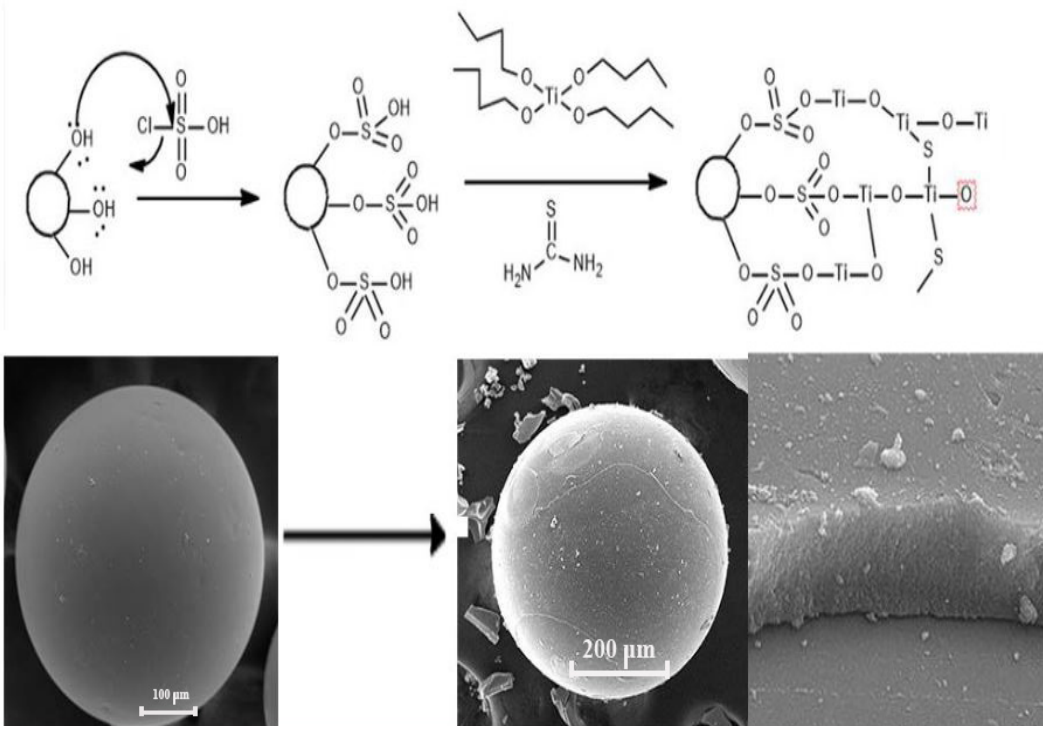

Figure 1. Schematic diagram of N,S-TiO_2 thin layer film coated on silica sulfuric acid

5, 15, 25, 40, 50 mg/L. The solutions were prepared to replicate each concentration at least three times, and only one catalyst bed was recycled for each of the three replicates. Each usage was followed by washing the catalyst multiple times with distilled water, sonicating, and drying in an oven at 90°C for 90 min and using it again. The glass MS containing N,S-TiO_2/SSA thin layer is distributed in four optical quartz tubes (0.8 cm in inner diameter and 20 cm in height). They are then exposed to visible light in a dark room (70×70×100 cm) using a 400 W lamp source. Then, 4.5 g of glass MS containing N,S-TiO_2/SSA thin film was used in each phototube. Next, they were immobilized in a mirror. There was a 20 cm distance between glass tubes and lamps in the dark chamber. An air conditioner pump and a cold water tank, including a valve, were employed to maintain constant

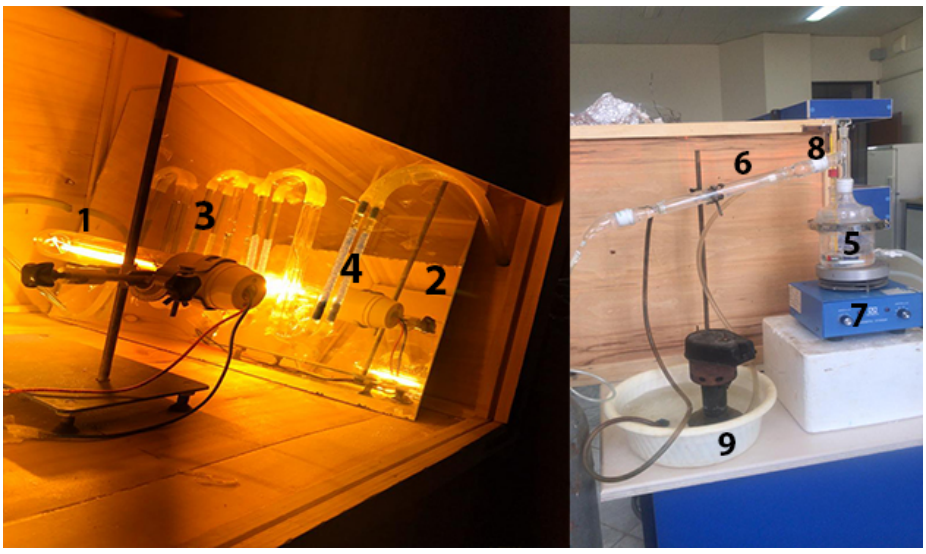

Figure 2. Plan of the pilot for this study

1) Light, 2) Mirror, 3) Photoreactor, 4) N,S-TiO_2 coated on SSA glass MS, 5) Reactor containing 1-naphthol solution, 6) Condenser, 7) Magnetic stirrer, 8) Thermometer, 9) Chiller pump and cold water chamber

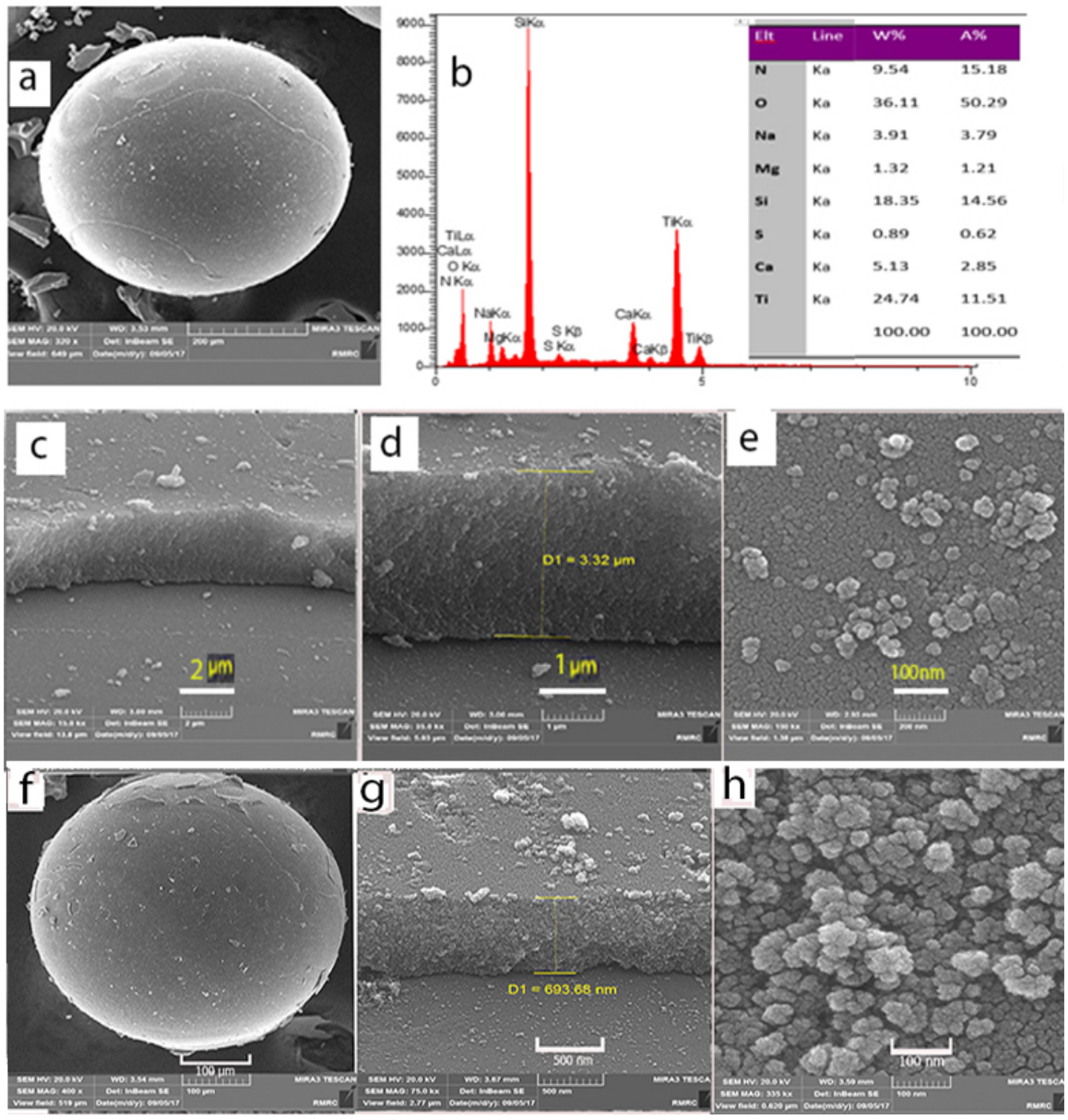

Figure 3. Energy-Dispersive X-ray (EDX) spectrum and Scanning Electron Microscope (SEM) images associated with N,S-TiO_2 coated on Silica Sulfuric Acid (SSA) and N,S-TiO_2 coated on pure glass Microspheres (MS), respectively

a) SEM image of N,S-TiO_2 coated on SSA; b) EDX analysis of N, S-TiO_2 coated on SSA; c) SEM image of a uniform thin film of N,S-TiO_2 coated on SSA; d) The thickness of N,S-TiO_2/SSA thin film (3.32 µm); e) Nanometer-sized N, S-TiO_2 particles on SSA image with high resolution; f) SEM image of uniform N,S-TiO_2 coated on the surface of the pure glass MS; g) The 693-nm thick thin film of N,S-TiO_2 coated on the surface of the glass MS; h) High-resolution image of nanometer-sized N, S-TiO_2 particles coated on the glass MS.

the temperature at 30°C within the reactor. The heat of the lamp produced a maximum temperature of 40°C in the dark chamber. The reactor used for photocatalytic investigation is shown in Figure 2. Using a UV-Vis spectrophotometer (PerkinElmer, America), the remaining concentration of the 1-naphthol solution was obtained at a maximum wavelength of 213 nm. Then, the 1-naphthol degradation yield was computed via Equation 1.

$$1.\ \eta=\frac{C_0-C_t}{C_0}\times 100$$

C_0 is the 1-naphthol primary concentration, C_t is the 1-naphthol remaining concentration after time t, and η is the 1-naphthol elimination percentage. The trials were done triplicate, and the average value was considered.

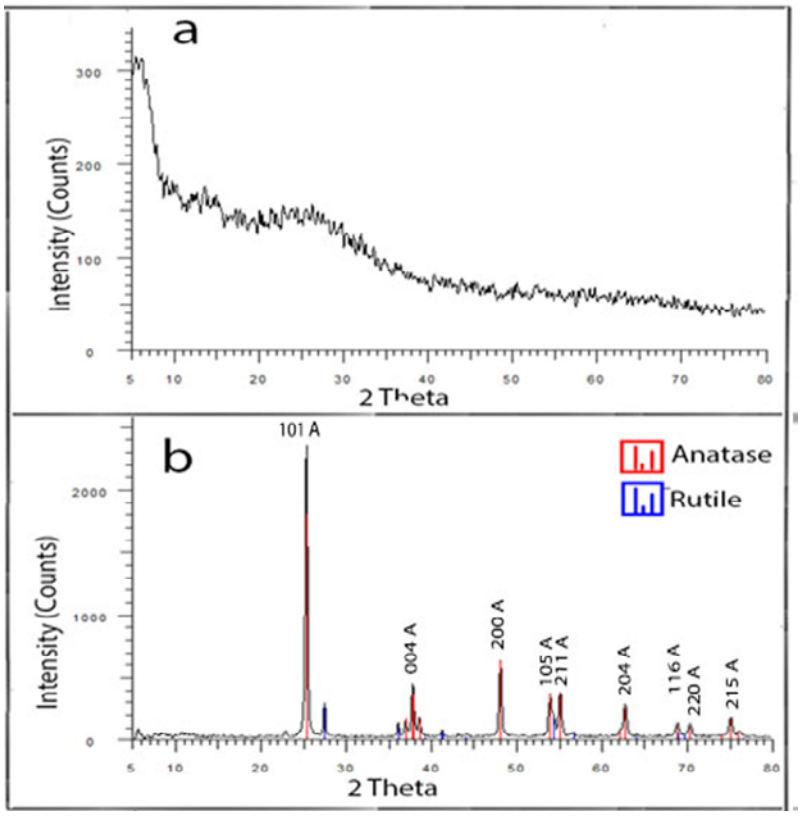

Figure 4. Thin film X-ray diffraction pattern

a) Image of pure Silica Sulfuric Acid (SSA) phase structure; b) image of N,S-TiO_2 thin film on SSA

1-naphthol extraction and Gas Chromatography-Mass Spectrometry (GC-MS) analysis

To recognize the intermediate compounds created by photo-oxidation reactions of 1-naphthol with N,S-TiO_2/SSA catalyst, 1-naphthol was extracted from an aqueous environment after irradiation, and the solution was injected into the Gas Chromatography-Mass Spectrometry (GC-MS) device [28]. We used a gas chromatography (Agilent Technologies 7890A model GC) device connected to the mass spectrometer (Agilent Technologies 5975C model) with a 30 m long, 0.25 m in outer diameter, and 0.25 in inner diameter HP5-MS column. As a carrier, helium was applied at a flow rate of 2 mL/min. Then, a total volume of 0.1 µL of the extracted solution sample was injected into the GC-MS.

3. Results and Discussion

Properties of photocatalyst

To do the initial analysis and calculate the weight and atomic percentage of the elements contained in the N,S-TiO_2/SSA nanocatalyst, we employed EDX analysis. Figure 3, parts a and b show EDX analysis of N,S-TiO_2/SSA thin film. Also, Figure 3, parts c, d, and e display their corresponding SEM images. Figure 3, parts f, g, and h show SEM images of N,S-TiO_2 thin film on pure glass MS. Figure 3b shows the peaks of the N,S-TiO_2 thin film coated on SSA, confirming the existence of Ti and Si in the presence of N and S in the TiO_2 thin film structure. It is noteworthy that the presence of magnesium, sodium, and calcium elements in the EDX analysis spectrum is associated with the glass MS structure. EDX analysis (Figure 3b) displays the peaks associated with the presence of N at 0.5 keV and S at 2.2 keV. The peak of Ti is exhibited at about 4.5-5 keV. As shown in Figure 3b, the elemental analysis of N,S-TiO_2/SSA thin film indicates that the sample is composed of oxygen (36.11 wt%), silicon (18.35 wt.%), sodium (3.91 wt%), magnesium (1.32 wt%), calcium (5.13 wt%, which can be attributed to glass MS), titanium (24.74 wt.%), sulfur (0.89 wt%), and nitrogen (9.54 wt%), indicating the presence of doped N,S atoms in the new TiO_2 photocatalytic layer. The EDX analysis results show that the percentage of sulfur atoms in the N,S-TiO_2/SSA catalyst is higher than that of the N,S-TiO_2 coated on pure glass MS, which can be attributed to the existence of sulfuric functional groups containing sulfur atoms on SSA. Figure 3, parts c, d, and e show the SEM images of N,S-TiO_2/SSA.

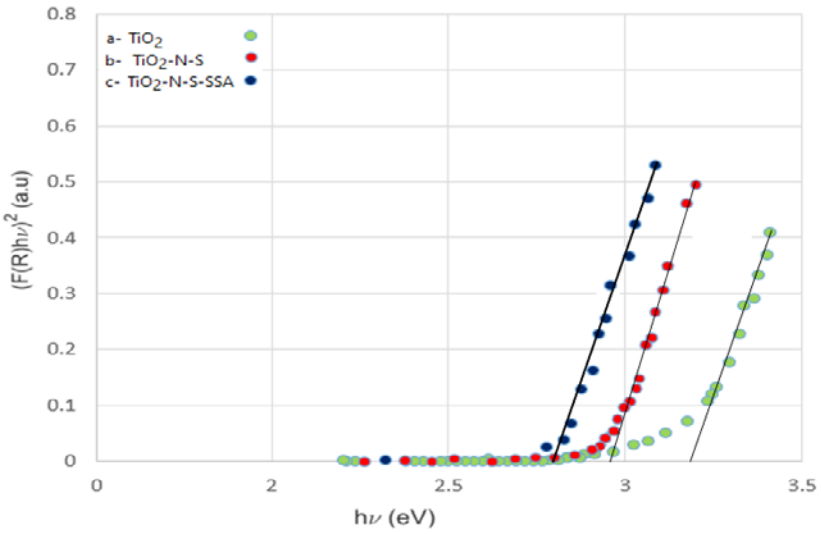

Figure 5. Differential Reflectance Spectroscopy (DRS) spectrum of pure TiO_2 and N,S-TiO_2/SSA thin film; DRS spectrum of pure TiO_2 (green line), (b) N,S-TiO_2 thin film on glass beads (red line), and (c) N,S-TiO_2/SSA thin film (blue line)

Compared to the previous studies, the thickness of N,S-TiO_2 thin film coated on SSA (3.32 µm) is higher than that of N,S-TiO_2 thin film coated on pure glass MS (809.93 nm) (Figure 3g). The sulfonic acid groups made a covalent bond with a hydroxyl group on the glass MS surface. The hydroxyl group of sulfuric acid on the surface of the glass MS establishes a good interaction with the prepared sol of tetrabutyl orthotitanate via hydrogen bonding. As a result, a thicker layer of N,S-TiO_2 immobilized on the surface of the SSA is created and causes the 1-naphthol molecule to be more adsorbed on the catalyst surface and increases the time required for the photocatalytic degradation process on the surface. Figure 3e illustrates the 5-10 nm nanosized N,S-TiO_2 particles coated on SSA, which are smaller than the nanosized N,S-TiO_2 particles coated on pure glass MS, i.e., 35-50 nm.

Figure 4 parts a and b display the XRD pattern of pure SSA and N-S-TiO_2/SSA, respectively. Figure 4a illustrates the XRD pattern of pure SSA, showing the amor-

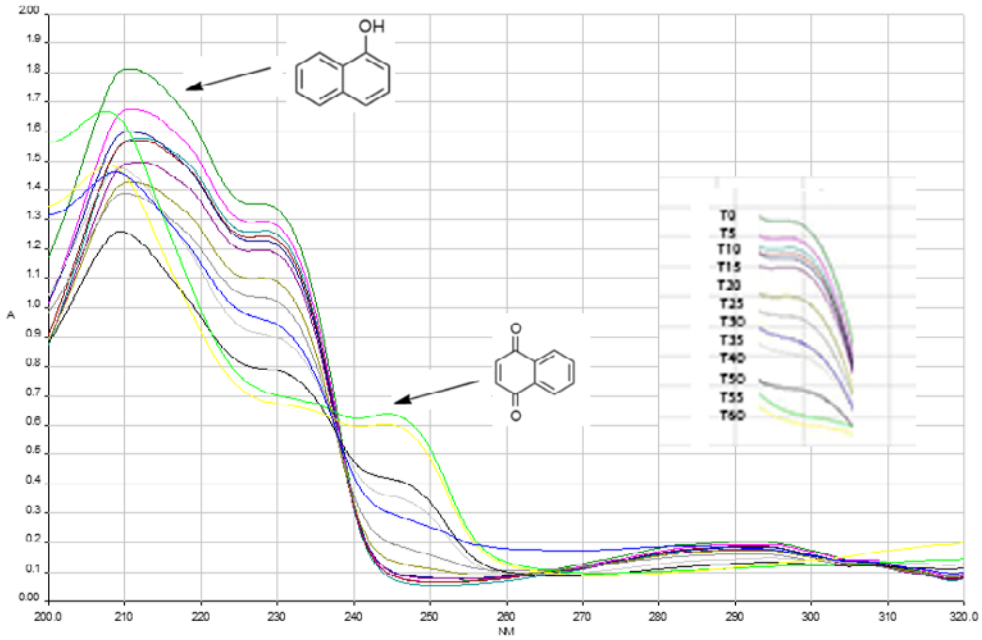

Figure 6. UV-Vis spectrum of 1-naphthol solution samples under N,S-TiO_2/SSA degradation reaction at specific times (0-60 min): pH=5, 1-naphthol concentration=5 mg/L under visible light

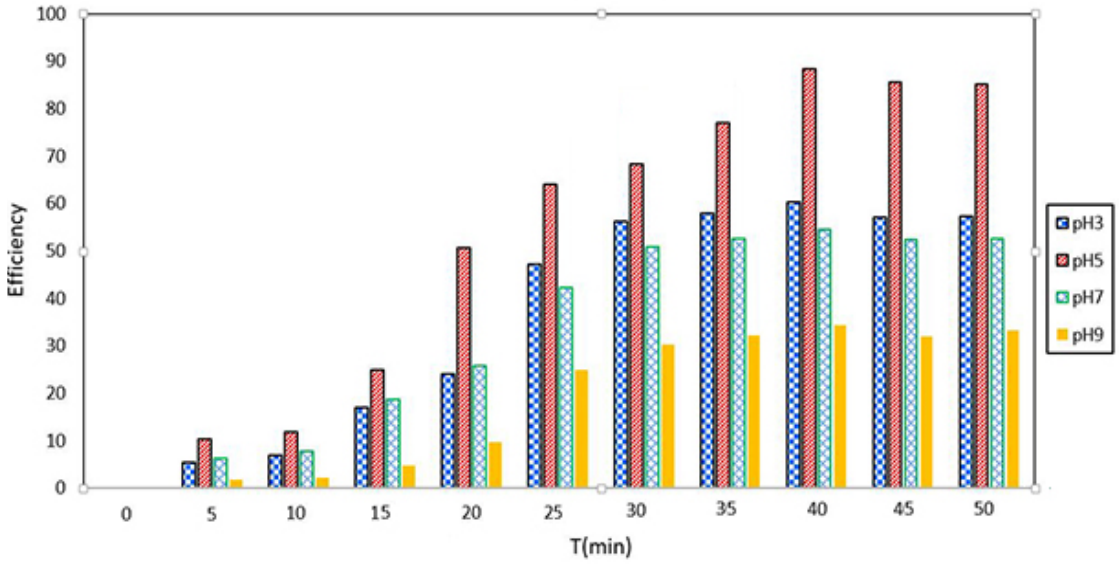

Figure 7. pH effect on removal efficiency of 1-naphthol (pH=5, P<0.05)

phous solid (blank). The XRD pattern of Ti element in synthesized photocatalyst is shown in Figure 4b for the anatase phase (red line) and rutile (blue line) phase, respectively. The crystal nanoparticles' average size in N,S-TiO_2 thin film-coated at peak 101 Å on SSA (based on XRD pattern) was obtained at 10 nm via the Scherrer equation. The characteristic peak at 2θ was obtained to be 25.348, signifying the anatase phase, and the characteristic peak at 2θ=27.32 is a trace of the rutile phase in the structure of N,S-TiO_2 coated on SSA. The comparison of the XRD results of N,S-TiO_2/SSA, and N,S-TiO_2 coated on the glass MS indicates that the rutile phase is observed in the N,S-TiO_2/SSA structure, while no rutile phase is seen in the N,S-TiO_2 catalyst immobilized on the glass MS.

Differential Reflectance Spectroscopy (DRS) spectrum analysis of pure TiO_2 and N,S-TiO_2/SSA is displayed in Figure 5. Tauc plot technique (Tauc) was used to calculate the nanostructures' optical bandgap energy using the Kubelka-Munk model [29]. These separately measured values were equal to an energy gap of 2.72 eV for N,S-TiO_2/SSA thin film, 3.2 eV for TiO_2 thin film, while the energy gap for the thin film of N,S-TiO_2 coated on glass MS is 2.98 eV [22]. As can be observed, the effect of the addition of sulfur and nitrogen to the TiO_2 crystal structure causes a narrower energy gap and transfers the TiO_2 photocatalytic activity to the visible region [30]. The comparison of the energy gap of N,S-TiO_2/SSA (2.72 eV) and N,S-TiO_2 coated on glass MS (2.98 eV) shows that the activity of N,S-TiO_2/SSA in the visible light will be greater than that of the N,S-TiO_2 coated on glass MS.

Photocatalytic degradation of 1-naphthol

Figure 6 shows the overlay UV-Vis spectrum of 1-naphthol concentration removal within 60 minutes (0-60). It should be noted that 1-naphthol has two maximum wavelengths of 213 nm and 230 nm. As a result, from the 55th minute onwards, the overall shape of the spectrum changes, showing the production of products other than 1-naphthol. It was found that from the 55 minutes onwards, the 1-naphthol molecule was converted to another intermediate product. The optimal time for 1-naphthol elimination via this photocatalyst was thus evaluated within 50 minutes. All statistical calculations for removing the 1-naphthol were then considered for up to 50 minutes. To identify the produced compounds in photodegradation, the samples were injected into GC-MS. All kinetic results between adsorption and concentration at 213 nm have been achieved due to the linear relationship between absorbance and 1-naphthol concentration at 213 nm based on Beer Lambert's law.

To obtain the optimum pH factor for 1-naphthol degradation, the impact of different pH values on the removal efficiency of 1-naphthol under visible light was investigated. The preparation of samples with a primary 1-naphthol solution concentration of 5 mg/L was done at pH values of 3, 5, 7, and 9. The samples were obtained and investigated at times of 0, 5, 10, 15, 20, 25, 30, 35, 40, 45, and 50 min on the catalyst's surface. To eliminate the effect of adsorption on removing 1-naphthol, all solutions were rotated for 45 minutes without the presence of light in the chamber. Then, according to the standard method,

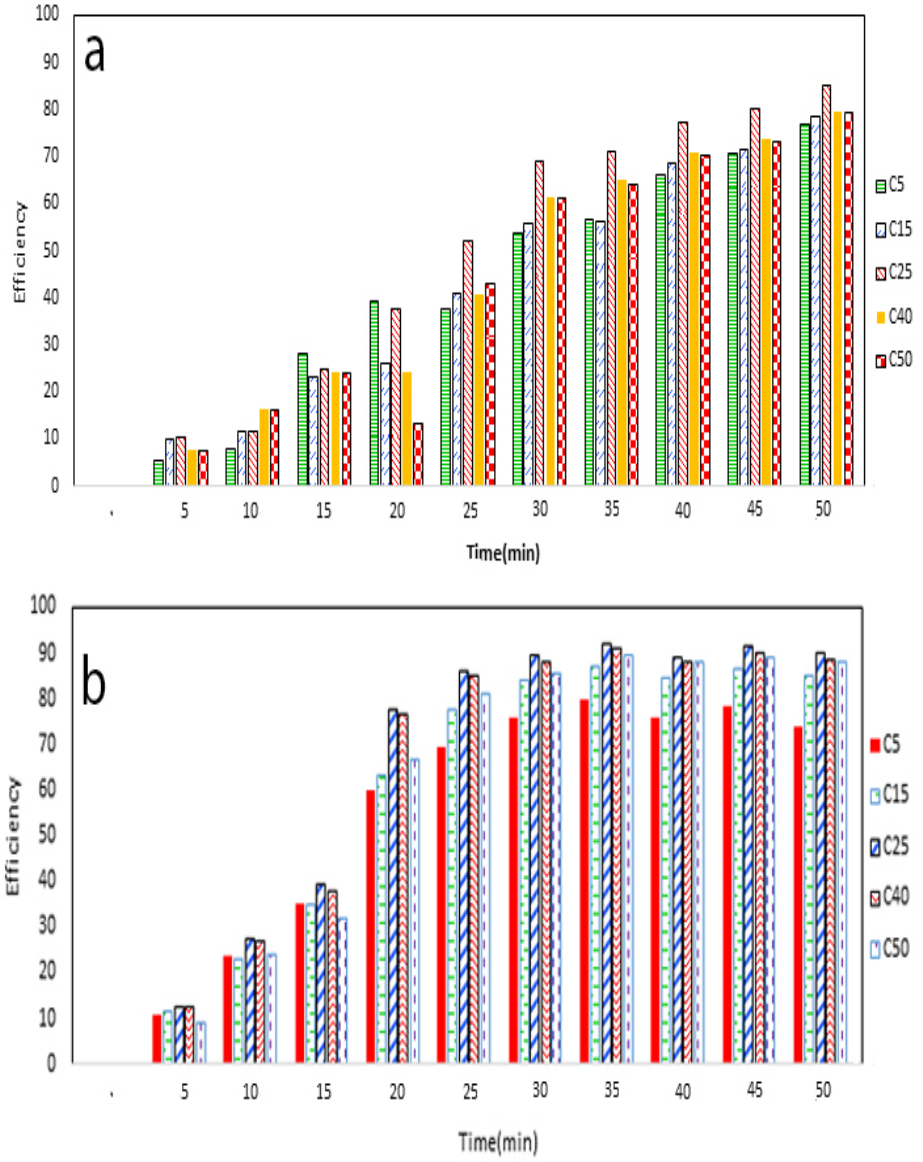

Figure 8. The 1-naphthol degradation efficiency at different Initial concentrations under visible light (5, 15, 25, 40, and 50 mg/L) in the exposure to N,S-TiO_2 coated on glass MS (a) and N,S-TiO_2/SSA (b) under visible light within 50 minutes

the samples absorption rate was read using a spectrophotometer at 213 nm, and the removal percentage of 1-naphthol was calculated by Equation 1. The results are shown in Figure 7. According to Figure 7, the optimum pH factor for degradation of 1-naphthol is equal to 5. The higher removal efficiency of 1-naphthol happens in an acidic environment owing to the accelerated formation of hydroxyl radicals and being absorbed on the N,S-TiO_2 nanocatalyst surface. The 1-naphthol contains hydroxyl groups that TiO_2 can absorb. TiO_2 surface is thus positively charged and easily exposed to photo-oxidation, but in the basic pH conditions, the TiO_2 surface is negatively charged, the hydroxyl functional group 1-naphthol is converted to hydroxyl anion and repels TiO_2.

Then, 1-naphthol solutions were made with concentrations of 5, 15, 25, 40, and 50 mg/L at constant pH of 5 (as optimum pH). Figure 8 shows the greatest concentration of 1-naphthol removal obtained under visible light at 25 mg/L for N,S-TiO_2 coated on glass MS with efficiency removal of 71% (8a) and 25 mg/L for N,S-TiO_2/SSA with efficiency removal of 92.12% (8b) ($P<0.05$).

Kinetic of 1-naphthol photocatalytic degradation

The kinetic of 1-naphthol degradation by N,S-TiO_2/SSA was shown to follow the quadratic Equation 2.

$$2.\ \frac{1}{C_t}-\frac{1}{C_0}=Kt$$

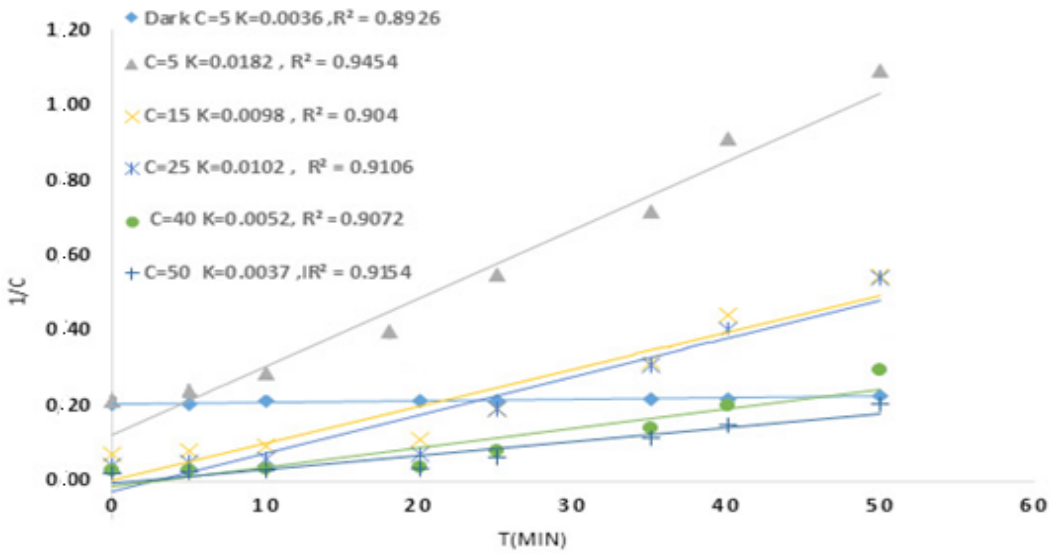

Figure 9. The second-order kinetic curve for degradation of 1-naphthol at various concentrations in the exposure to N,S -TiO_2/ SSA and visible light

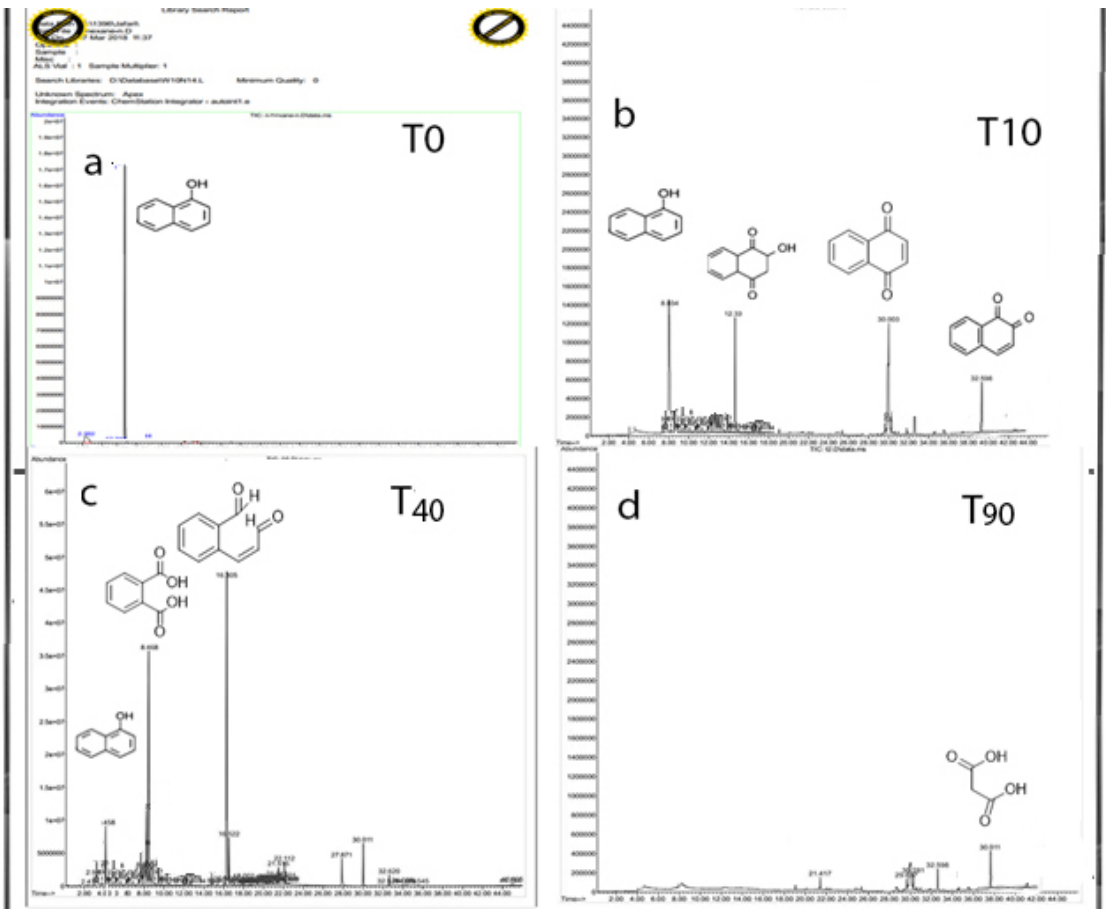

Figure 10. Intermediate compounds formed from 1-naphthol photo-oxidation by N,S-TiO_2/SSA catalyst during irradiation At: a) time=0; b) time=10 min; c) time=40 min; and d) time 90 min.

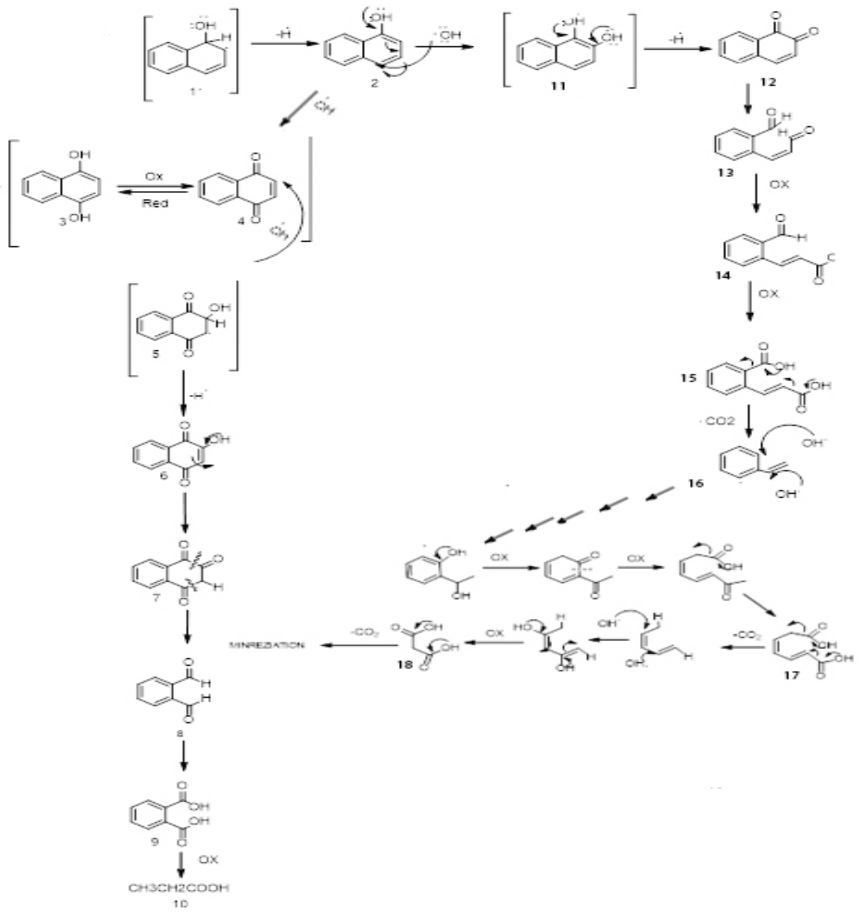

Figure 11. Intermediate compounds formed from 1-naphthol photo-oxidation by N,S-TiO_2/SSA catalyst

Where, t is the time of reaction (minute), K shows reaction rate constant (1/min), and C_0 and C_t denote the primary and secondary concentration of 1-naphthol post-reaction in mg/L at t=0 and t=t, respectively.

The contact time was changed up to 50 min with different concentrations of 1-naphthol in the exposure of N,S-TiO_2/SSA to perform the kinetics experiments. Using the correlation coefficient, the proportionality of the regression equation of the samples with the data was displayed. By comparing between R^2 coefficients of all samples, the kinetic model analysis of 1-naphthol degradation was carried out. Figure 9 shows the kinetics graphs of 1-naphthol removal in 1/C versus irradiation time. Considering the line 1/C slope versus time, the rate constants were obtained. The R^2 regression coefficient for the second-order kinetic graph was greater than 0.9. It is noteworthy that in the present study, the total time of 1-naphthol removal is 50 min. This result is evident because the 1-naphthol adsorption pattern disappears entirely within 50 minutes. From 50 min onward, the quinoline compound is characterized by adsorption spectrum as an intermediate because of the optical decomposition of 1-naphthol. The 1-naphthol kinetic reaction was thus investigated from 0 to 50 min and assessed based on the second-order kinetics. The previous literature has reported photo-oxidation degradation kinetics of 1-naphthol during degradation time and they report second order kinetics which is in good agreement with the results of this study [31-33].

Catalyst reusability

The N,S-TiO_2/SSA reusability was investigated for the 1-naphthol degradation at a primary concentration of 25 mg/L under visible light. The catalyst was used five times, and the results of 1-naphthol degradation show the ability to stabilize light as a percentage of 1-naphthol degradation under visible light. After the destruction was completed, the catalyst was isolated and washed with an excess of deionized water.

Intermediate compounds produced through naphthalene degradation

Using Agilent 5975C model GC-MS, we investigated the intermediate compounds produced through 1-naph-

Table 1. Efficiency of 1-n aphthol removal by conventional processes

Material	Process / Mechanism	Experimental/Optimal conditions	Efficiency (%)	Ref.
N,S-TiO_2/SiO_2/UV	Photo catalytic degradation	Optimal pH=5, time=50 min, concentration C_0= 25 mg/L	Removal= 92.12% of 1-naphthol within 50 min	Present Study (2021)
Fe-N-S-MPC	Oxidation	Fe-N-S-SMPC: $[Fe\text{-}N\text{-}S\text{-}MPC]_0$ = 75 mg/L, $[PMS]_0$ = 25 mg/L, [1-naphthol] = 20 mg/L, pH = 2.5	Removal= 90% of 1-naphthol within 30 min	[34]
β-cyclodextrin modified graphene oxide nanosheets (β-CD-GO)	Adsorption	pH = 2-12, C0=36 mg/L Time=20-350 min T=293 K	adsorption capacity: 207.6 mg/g at 293 K	[35]
Zeolitic imidazolate framework-67 (ZIF-67)	Adsorption	pH =8 V=0.05 L, ZIF-67=100 mg/L, T=293 K, 303 K, 313 K	adsorption capacity: 339 mg/g at 313 K	[36]
carbon nanotubes/iron oxides (MWCNTs/iron)	Oxidation\ Adsorption	C_0 = 120 pH = 7.0, T = 293 K.	qmax (mg/g), 293 K at First time: 105.43±4.63 and Second time: 71.93±6.05 with Longmuir model Removal: 96.9%	[37]
Fe3O4@cyclodextrin (Fe3O4@CD MNPs)	Oxidation\ Adsorption	T = 293 K, m/V = 0.5 g/L, C1-naphthol = 50 mg/L, I = 0.01 mol/L NaCl., pH = 2-12	Removal: 41% at pH = 9 and real effluent	[38]
reduced graphene oxide (rGO)	Adsorption	h-Rgo=0.1 mg/mL, Temp =50 °C, Time= 5 day, C0 = 0.1-3 mmol/L	At 303 K, qmax values of l-rGO =3.57 and h-rGO = 5.55 mmol/g , at 323 K, the qmax of h-rGO for 1-naphthol is 8.6 mmol/g	[39]
ZnO and TiO_2 /UV	Photo catalytic degradation	Oxide loading= 0.10 g, airflow= 7.8 mL/s, dissolved O_2=19.2 mg/L, 365 nm, 19.2_Einstein 1/Ls, 1-naphthol solution=20 mL	ZnO wurtzite and TiO_2 anatase effectively catalyze degradation of 1-naphthol under UV light TiO_2=92% ZnO=100%	[40]

thol photodegradation in the exposure of N,S-TiO_2/SSA. For this purpose, the samples were extracted by dichloromethane solvent and then injected into GC-MS. Figure 10 shows the GC spectrum for intermediate compounds produced from photo-oxidation of 1-naphthol using N,S-TiO_2/SSA catalyst during irradiation at 0, 10, 40, and 90 minutes. The intermediate compounds were described by considering the retention time and device library assessment based on the interpretation of the mass spectrum. Jafari et al. [22] reported 1-naphthol as one of the intermediate compounds produced post naphthalene photo-oxidation. They proposed the oxidation mechanism by OH radicals for 1-naphthol removal, which corresponds to the compounds identified from the mass spectrum in this study. The photo-oxidation mechanism for 1-naphthol removal in the presence of OH radicals is presented in Figure 11.

The intermediate compounds include phthalic acid (9), 1, 2-naphthalenedione (12) 1, 4-naphthalenedione (4) and 2-carboxy-cinnamaldehyde (13). The GC-MS results after 90 minutes confirmed the removal of many intermediates and their eventual conversion to CO_2 and H_2O gases (Figure 11).

Studies on the removal of naphthalene have been performed by various methods, as shown in Table 1. Adsorption, oxidation, and photocatalytic processes are common methods in that order.

4. Conclusion

In this study, N,S-TiO_2/SSA photocatalyst synthesis was successfully performed using the sol-gel method. The SEM analysis revealed the nanosized thin film of N,S-TiO_2/SSA to be about 5-10 nm. Moreover, the DRS results of N,S-TiO_2/SSA indicated the reduction of the energy gap (0.48 eV). The obtained results indicated that the energy gap band was narrowed, and the N,S-TiO_2/SSA optical activity was directed towards visible light. The results of the study of 1-naphthalene solutions at various concentrations in the exposure of N,S-TiO_2/SSA show that the kinetic equation of 1-naphthol removal follows the second-order model and the best removal conditions of 1-naphthol happen at pH=5, 1-naphthol

primary concentration of 25 mg/L, under visible light within 50 minutes. The maximum removal efficiency of 1-naphthol under visible light was 92.12%. The GC/MS study results show the production of some intermediate compounds that are mineralized after another 100 minutes of contact time. It is suggested that the efficiency of N,S-TiO_2/SSA photocatalysis for eliminating the total polycyclic aromatic hydrocarbons.

Ethical Considerations

Compliance with ethical guidelines

There was no ethical consideration to be considered in this research.

Funding

This study was supported by Ahvaz Branch, Islamic Azad University, Ahvaz.

Authors' contributions

Conceptualization and Supervision: Farhad Mahmoodi: Study design and concept, literature review, structuring; Methodology: Farhang Tirgir and Mehraban Sadeghi; Data analysis and Writing-original draft, and Writing-review & editing, and project administration: Jalilzadeh.

Conflict of interest

The authors declared no conflict of interest.

Acknowledgments

The authors would like to thank the Research Council for their generous support regarding this research.

References

[1] Chen X, Vione D, Borch T, Wang J, Gao Y. Nano-MoO_2 activates peroxymonosulfate for the degradation of PAH derivatives. Water Res. 2021; 192:116834. [DOI:10.1016/j.watres.2021.116834] [PMID]

[2] Liu Y, Zhu M, Hu Y, Zhao Y, Zhu C. Photochemical reaction of superoxide radicals with 1-naphthol. Can J Chem. 2021; 99(11):867-73. [DOI:10.1139/cjc-2021-0028]

[3] Cerniglia CE, Freeman JP, Evans FE. Evidence for an arene oxide-NIH shift pathway in the transformation of naphthalene to 1-naphthol by Bacillus cereus. Arch Microbiol. 1984; 138(4):283-6. [DOI:10.1007/BF00410891] [PMID]

[4] Croera C, Ferrario D, Gribaldo L. In vitro toxicity of naphthalene, 1-naphthol, 2-naphthol and 1,4-naphthoquinone on human CFU-GM from female and male cord blood donors. Toxicol In Vitro. 2008; 22(6):1555-61. [DOI:10.1016/j.tiv.2008.06.004] [PMID]

[5] Orooji N, Takdastan A, Yengejeh RJ, Jorfi S, Davami AH. Photocatalytic degradation of 2, 4-dichlorophenoxyacetic acid using Fe 3 O 4® TiO 2/Cu 2 O magnetic nanocomposite stabilized on granular activated carbon from aqueous solution. Res Chem Intermediates. 2020; 46(5):2833-57. [DOI:10.1007/s11164-020-04124-9]

[6] Yang L, Gong R, Waterhouse GIN, Dong J, Xu J. A novel covalent triazine framework developed for efficient determination of 1-naphthol in water. Environ Sci Pollut Res Int. 2021; 28(24):31185-94. [DOI:10.1007/s11356-021-12869-y] [PMID]

[7] Rengaraj S, Li XZ. Enhanced photocatalytic activity of TiO_2 by doping with Ag for degradation of 2, 4, 6-trichlorophenol in aqueous suspension. J Mol Catal A: Chem. 2006; 243(1):60-7. [DOI:10.1016/j.molcata.2005.08.010]

[8] Kazemi Noredinvand B, Takdastan A, Jalilzadeh Yengejeh R. Removal of organic matter from drinking water by single and dual media filtration: a comparative pilot study. Desalination Water Treat. 2016; 57(44):20792-9. [DOI:10.1080/19443994.2015.1110718]

[9] Ahmadpour E, Jalilzadeh Yengejeh R. Application of a zero-valente iron-per sulfate system to treat petrochemical wastewater with high-total dissolved solids containing parachlorophenol. Jundishapur J Health Sci. 2016; 8(2):e35108. [DOI:10.17795/jjhs-35108]

[10] Karimipour Z, Jalilzadeh Yengejeh R, Haghighatzadeh A, Mohammadi MK, Rouzbehani MM. UV-induced photodegradation of 2, 4, 6-trichlorophenol using ag-Fe 2 O 3-CeO 2 photocatalysts. J Inorg Organomet Polym Mater. 2021; 31(3):1143-52. [DOI:10.1007/s10904-020-01859-1]

[11] Bayati F, Mohammadi MK, Yengejeh R, Babaei AA. Ag2 O/GO/TiO_2 composite nanoparticles: Synthesis, characterization, and optical studies. J Aust Ceram Soc. 2021; 57(1):287-93. [DOI:10.1007/s41779-020-00528-3]

[12] Ho TNS, Nguyen TT, Pham THT, Ngo MH, Le MV. Photocatalytic degradation of phenol in aqueous solutions using TiO_2/SiO_2 composite. Chem Eng Trans. 2020; 78:427-32. https://www.aidic.it/cet/20/78/072.pdf

[13] Zangeneh H, Zinatizadeh AAL, Habibi M, Akia M, Isa MH. Photocatalytic oxidation of organic dyes and pollutants in wastewater using different modified titanium dioxides: A comparative review. J Ind Eng Chem. 2015; 26:1-36. [DOI:10.1016/j.jiec.2014.10.043]

[14] Zarrin S, Heshmatpour F. Photocatalytic activity of TiO_2/Nb2O5/PANI and TiO_2/Nb2O5/RGO as new nanocomposites for degradation of organic pollutants. J Hazard Mater. 2018; 351:147-59. [DOI:10.1016/j.jhazmat.2018.02.052] [PMID]

[15] Pandiyaraj KN, Vasu D, Ghobeira R, Tabaei PSE, De Geyter N, Morent R, et al. Dye wastewater degradation by the synergetic effect of an atmospheric pressure plasma treatment and the photocatalytic activity of plasma-functionalized Cu-TiO_2 nanoparticles. J Hazard Mater. 2021; 405:124264. [DOI:10.1016/j.jhazmat.2020.124264] [PMID]

[16] Derakhshan-Nejad A, Rangkooy HA, Cheraghi M, Yengejeh RJ. Removal of ethyl benzene vapor pollutant from the air using TiO_2 nanoparticles immobilized on the ZSM-5 zeolite un-

der UVradiation in lab scale. J Environ Health Sci Eng. 2020; 18(1):201-9. [DOI:10.1007/s40201-020-00453-4] [PMID] [PMCID]

[17] Swaminathan M, Shanthi M. Photocatalytic degradation of naphthol green b dye using coupled CdS-ZnMoO4 in UV-A light irradiation. J Nanosci Nanotechnol. 2021; 21(3):1526-36. [DOI:10.1166/jnn.2021.18984] [PMID]

[18] Fan J, Zhao Z, Liu W, Xue Y, Yin S. Solvothermal synthesis of different phase N-TiO_2 and their kinetics, isotherm and thermodynamic studies on the adsorption of methyl orange. J Colloid Interface Sci. 2016; 470:229-36. [DOI:10.1016/j.jcis.2016.02.045] [PMID]

[19] Lei XF, Xue XX, Yang H, Chen C, Li X, Pei JX, et al. Visible light-responded C, N and S co-doped anatase TiO_2 for photocatalytic reduction of Cr (VI). J Alloys Compd. 2015; 646:541-9. [DOI:10.1016/j.jallcom.2015.04.233]

[20] Khalilzadeh A, Fatemi S. Modification of nano-TiO 2 by doping with nitrogen and fluorine and study acetaldehyde removal under visible light irradiation. Clean Technol Environ Policy. 2014; 16(3):629-36. [DOI:10.1007/s10098-013-0666-7]

[21] Ghanbari A, Kashaninia A, Sadr A, Saghaei H. A comparative study of multipole and empirical relations methods for effective index and dispersion calculations of silica-based photonic crystal fibers. J Commun Eng. 2019; 8(1):93-103. [DOI:10.22070/JCE.2019.4016.1125]

[22] Jafari A, Sadeghi M, Tirgir F, Borghaei SM. Sulfur and nitrogen doped-titanium dioxide coated on glass microspheres as a high-performance catalyst for removal of naphthalene (C10H8) from aqueous environments using photo oxidation in the presence of visible and sunlight. Desalination Water Treat. 2020; 192:195-212. [DOI:10.5004/dwt.2020.25659]

[23] Saghaei H. Dispersion-engineered microstructured optical fiber for mid-infrared supercontinuum generation. Appl Opt. 2018; 57(20):5591-8. [DOI:10.1364/AO.57.005591] [PMID]

[24] Ebnali-Heidari M, Saghaei H, Koohi-Kamali F, Moghadasi MN, Moravvej-Farshi MK. Proposal for supercontinuum generation by optofluidic infiltrated photonic crystal fibers. J Sel Top Quantum Electron. 2014; 20(5):582-9. [DOI:10.1109/JSTQE.2014.2307313]

[25] Odling G, Pong ZY, Gilfillan G, Pulham CR, Robertson N. Bismuth titanate modified and immobilized TiO_2 photocatalysts for water purification: Broad pollutant scope, ease of reuse and mechanistic studies. Environ Sci Water Res Technol. 2018; 4(12):2170-8. [DOI:10.1039/C8EW00568K]

[26] Meng X, Zhang Z. Experimental analysis of a photoreactor packed with Pd-$BiVO_4$-Coated glass beads. AIChE J. 2019; 65(1):132-9. [DOI:10.1002/aic.16388]

[27] Zolfigol MA, Madrakian E, Ghaemi E. Silica sulfuric acid/$NaNO_2$ as a novel heterogeneous system for the nitration of phenols under mild conditions. Molecules. 2002; 7(10):734-42. [DOI:10.3390/71000734] [PMCID]

[28] Takeuchi A, Nakamura S, Namera A, Kondo T, Onuki H, Yamamoto S, et al. Simple and reliable method to simultaneously determine urinary 1-and 2-naphthol using in situ derivatization and gas chromatography-mass spectrometry for biological monitoring of naphthalene exposure in occupational health practice. J Occup Health. 2020; 62(1):e12144. [DOI:10.1002/1348-9585.12144]

[29] Pérez-Larios A, Lopez R, Hernandez-Gordillo A, Tzompantzi F, Gómez R, Torres-Guerra LM. Improved hydrogen production from water splitting using TiO_2-ZnO mixed oxides photocatalysts. Fuel. 2012; 100:139-43. [DOI:10.1016/j.fuel.2012.02.026]

[30] Saghaei H, Van V. Broadband mid-infrared supercontinuum generation in dispersion-engineered silicon-on-insulator waveguide. J Opt Soc Am B. 2019; 36(2):A193-202. [DOI:10.1364/JOSAB.36.00A193]

[31] Karuthapandian S, Arunsunaikumar K. Solar radiation catalyzed aerobic photooxidation of 1-naphthol on some semiconductors. Asian J Sci Appl Technol. 2014; 3(2):25-32. https://citeseerx.ist.psu.edu/viewdoc/download?doi=10.1.1.1072.9519&rep=rep1&type=pdf

[32] Sreekanth R, Prasanthkumar KP, Sunil Paul MM, Aravind UK, Aravindakumar CT. Oxidation reactions of 1-and 2-naphthols: An experimental and theoretical study. J Phys Chem A. 2013; 117(44):11261-70. [DOI:10.1021/jp4081355] [PMID]

[33] Mammeri L, Sehili T, Belaidi S, Djebbar K. Heterogeneous photodegradation of 1-naphthol with natural iron oxide in water: Influence of oxalic acid. Desalination Water Treat. 2015; 54(8):2324-33. [DOI:10.1080/19443994.2014.899928]

[34] Zhang T, Li C, Sun X, Gao H, Liu X, Sun J, et al. Iron nanoparticles encapsulated within nitrogen and sulfur co-doped magnetic porous carbon as an efficient peroxymonosulfate activator to degrade 1-naphthol. Sci Total Environ. 2020; 739:139896. [DOI:10.1016/j.scitotenv.2020.139896] [PMID]

[35] Zheng H, Gao Y, Zhu K, Wang Q, Wakeel M, Wahid A, et al. Investigation of the adsorption mechanisms of Pb (II) and 1-naphthol by β-cyclodextrin modified graphene oxide nanosheets from aqueous solution. J Colloid Interface Sci. 2018; 530:154-62. [[DOI:10.1016/j.jcis.2018.06.083] [PMID]

[36] Yan X, Hu X, Chen T, Zhang S, Zhou M. Adsorptive removal of 1-naphthol from water with Zeolitic imidazolate framework-67. J Phys Chem Solids. 2017; 107:50-4. [DOI:10.1016/j.jpcs.2017.03.024]

[37] Wang X, Chen C, Li J, Wang X. Ozone degradation of 1-naphthol on multiwalled carbon nanotubes/iron oxides and recycling of the adsorbent. Chem Eng J. 2015; 262:1303-10. [DOI:10.1016/j.cej.2014.10.107]

[38] Zhang X, Wang Y, Yang S. Simultaneous removal of Co (II) and 1-naphthol by core-shell structured Fe3O4@ cyclodextrin magnetic nanoparticles. Carbohydr Polym. 2014; 114:521-9. [DOI:10.1016/j.carbpol.2014.08.072] [PMID]

[39] Ali MM, Sandhya KY. Reduced graphene oxide as a highly efficient adsorbent for 1-naphthol and the mechanism thereof. RSC Adv. 2014; 4(93):51624-31. [DOI:10.1039/C4RA05702C]

[40] Karunakaran C, Narayanan S, Gomathisankar P. Photocatalytic degradation of 1-naphthol by oxide ceramics with added bacterial disinfection. J Hazard Mater. 2010; 181(1-3):708-15. [DOI:10.1016/j.jhazmat.2010.05.070] [PMID]

This Page Intentionally Left Blank